

Supplementary data

Table S1. Input parameters predicted from chemical structure for GastroPlus™ simulation

Parameters	Values
Molecular weight (g/mol)	576.73
Log P	2.8
Human jejunal permeability ($\times 10^{-4}$ cm/s)	1.89
Reference solubility at pH 7 (mg/mL)	0.0282
Biorelevant solubilities (mg/mL)	
SGF (pH 1.2)	0.0356
FaSSIF (pH 6.5)	0.0288
FeSSIF (pH 5.0)	0.15
Diffusion coefficient ($\times 10^{-5}$ cm ² /s)	0.51
Blood/plasma concentration ratio	0.83
Plasma unbound fraction (%)	8.71

SGF, simulated gastric fluid; FaSSIF, fasted state simulated intestinal fluid; FeSSIF, fed state simulated intestinal fluid.

Table S2. Comparison of the ¹H NMR data of cerberin (CR) isolated in this study and data reported for cerberin [30] and neriifolin [31]

	CR (CD ₃ OD, 600 MHz) δ (ppm), mult (<i>J</i> in Hz)	Cerberin (CDCl ₃ , 600 MHz) δ (ppm), mult (<i>J</i> in Hz)	Neriifolin (CDCl ₃ , 250 MHz) δ (ppm), mult (<i>J</i> in Hz)
18	0.98, 3H, s	0.90, 3H, s	0.88, 3H, s
19	1.20, 3H, d (6.3)	0.98, 3H, s	0.97, 3H, s
6'	0.88, 3H, s	1.30, 3H, d (6)	1.26, 3H, d (6.3)
C2'-O- <u>Ac</u>	2.05, 3H, s	2.08, 3H, s	-
17	2.83, 1H, dd (5.7, 9.1)	2.80, 1H, m	2.78, 1H, dd (5.0, 8.8)
4'	3.08, dd (9.4, 9.4)		3.15, 1H, dd (9.0, 9.0)
3'	3.50, dd (9.2, 9.8)		3.25, 1H, dd (8.9, 8.9)
3	3.88, 1H, m		3.97, m
3'-O- <u>CH₃</u>	3.57, 3H, s	3.64, 3H, s	3.69, 3H, s
2'	4.51, 1H, dd (3.8, 10.0)	4.72, dd (4, 10)	3.58, 1H, dd (4.4, 8.9)
5'	3.73, 1H, dq (6.3, 9.4)		3.74, 1H, dq (9.0, 6.3)
21	4.82, 1H, dd (1.5, 18.2)	5.00, 2H, dd (3, 6)	4.82, 1H, dd (1.5, 18.0)
	4.98, 1H, dd (1.5, 18.2)		4.98, 1H, dd (1.5, 18.0)
1'	5.01, 1H, d (3.8)	5.12, 1H, d (4)	4.86, 1H, d (4.4)
22	5.89 1H, t (1.5)	5.97, 1H, bs	5.88, 1H, t (1.5)

NOT-CO-1 CD3OD 1H

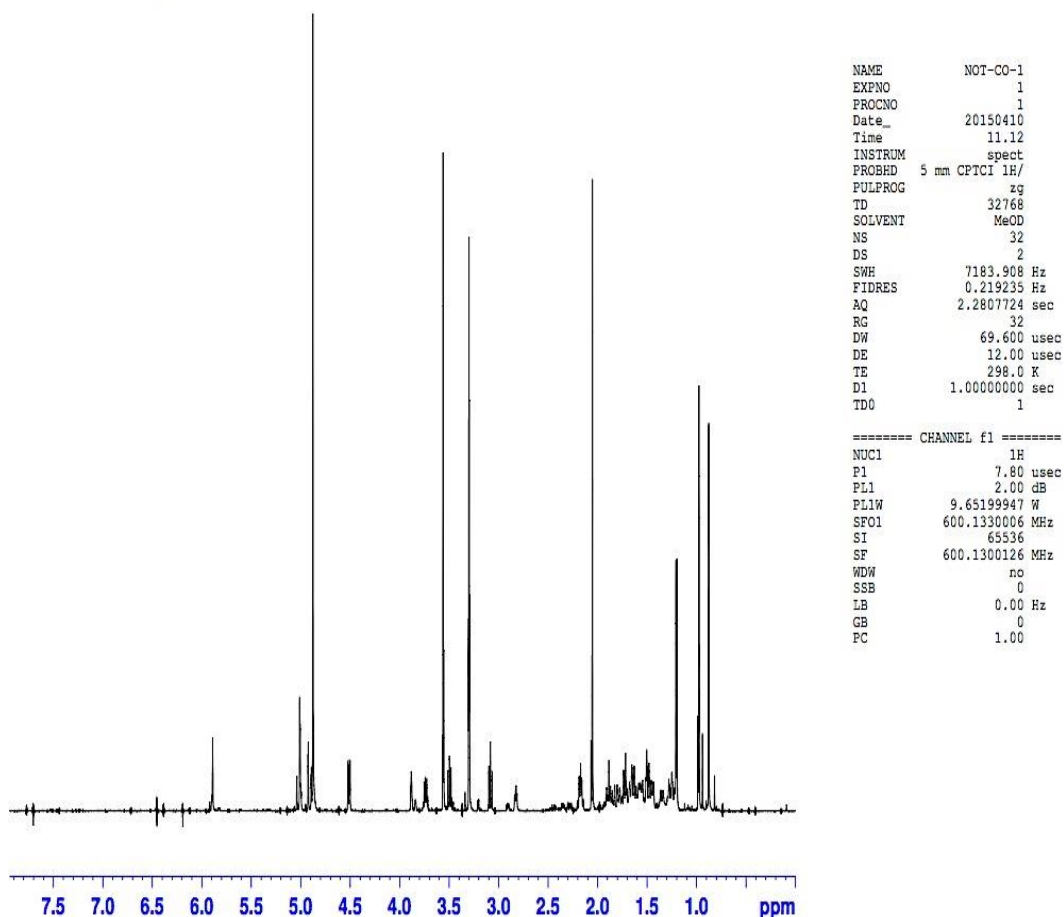


Figure S1. ^1H NMR spectra of the isolated compound, cerberin.

Sample identified as Cerberin (IUPAC: [(2*R*,3*S*,4*R*,5*S*,6*S*)-5-Hydroxy-2-[[[(3*S*,5*R*,8*R*,9*S*,10*S*,13*R*,14*S*,17*R*)-14-hydroxy-10,13-dimethyl-17-(5-oxo-2*H*-furan-3-yl)-1,2,3,4,5,6,7,8,9,11,12,15,16,17-tetradecahydrocyclopenta[*a*]phenanthren-3-yl]oxy]-4-methoxy-6-methyloxan-3-yl] acetate).

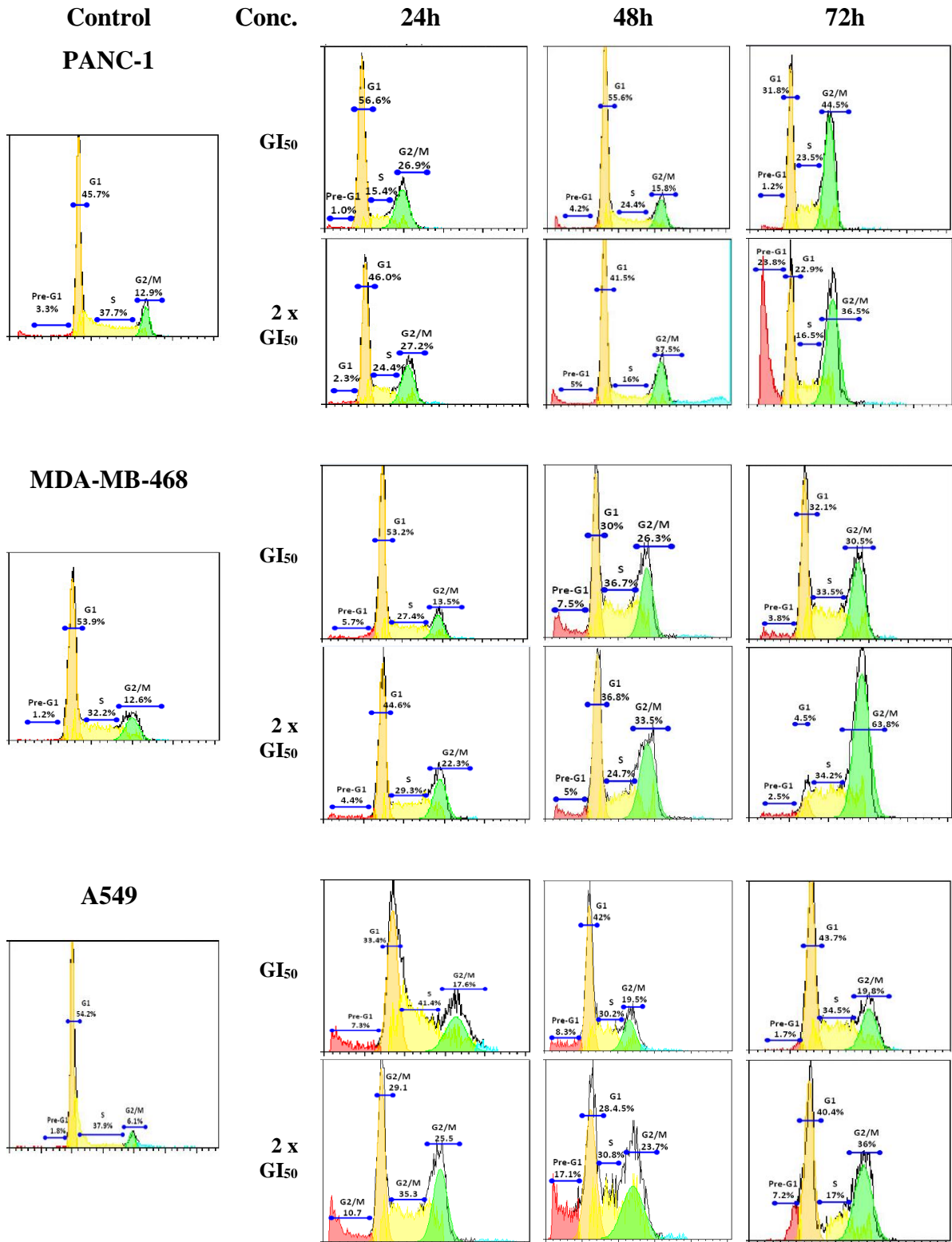


Figure S2. Representative cell cycle histograms from a single trial of PANC-1, MDA-MB-468 and A549 cells treated with CR at respective 1 x GI₅₀ and 2 x GI₅₀ concentrations for 24 h, 48 h and 72 h.

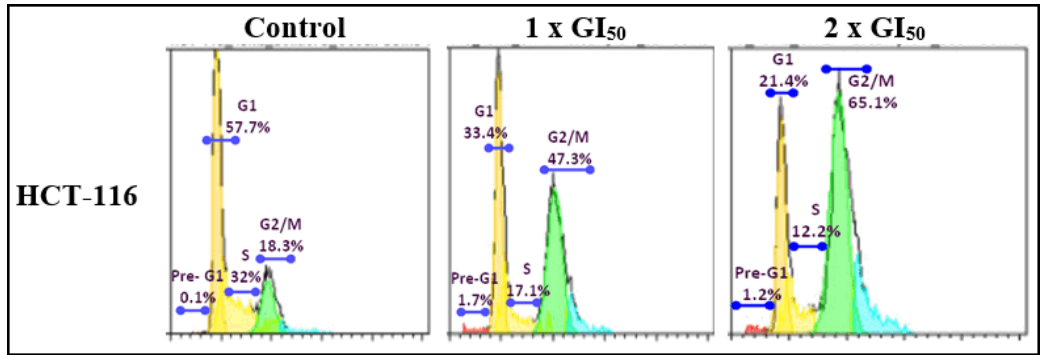


Figure S3. Representative cell cycle histograms from a single trial of HCT-116 cells treated with CR at respective 1 x GI₅₀ and 2 x GI₅₀ concentrations for 48 h.

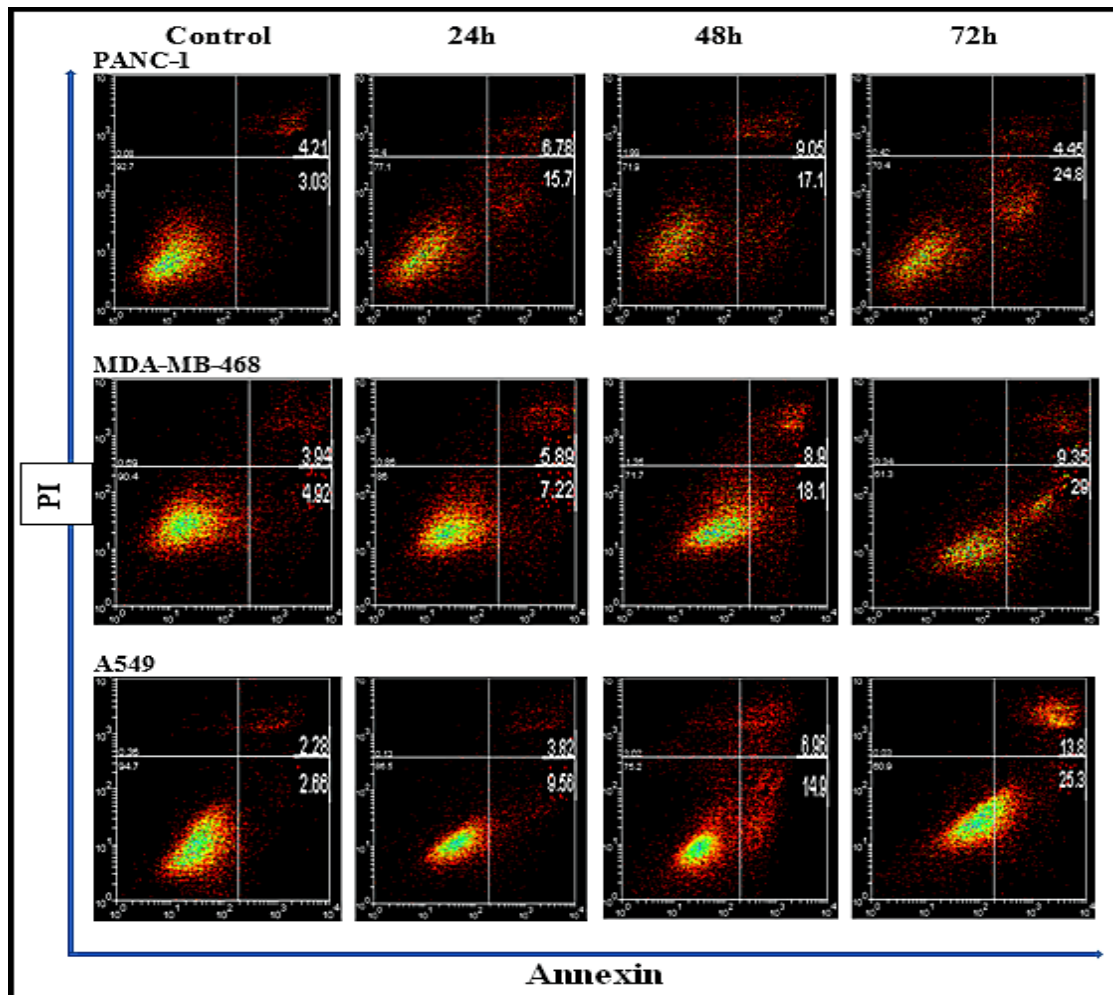


Figure S4. Representative apoptosis quadrant plots illustrating apoptotic effects of CR.

PANC-1, MDA-MB-468, A549 and HK-1 cells were treated with 1x GI₅₀ and 2x GI₅₀ concentrations of CR for 24 h, 48 h, and 72 h. These are representative quadrant plots analysed

by flow cytometry, 15,000 events were recorded for each experiment. Lower right quadrant contains the early apoptotic (Annexin+/PI-) population and the upper right quadrant contain the late apoptotic or necrotic (Annexin +/PI+) populations.

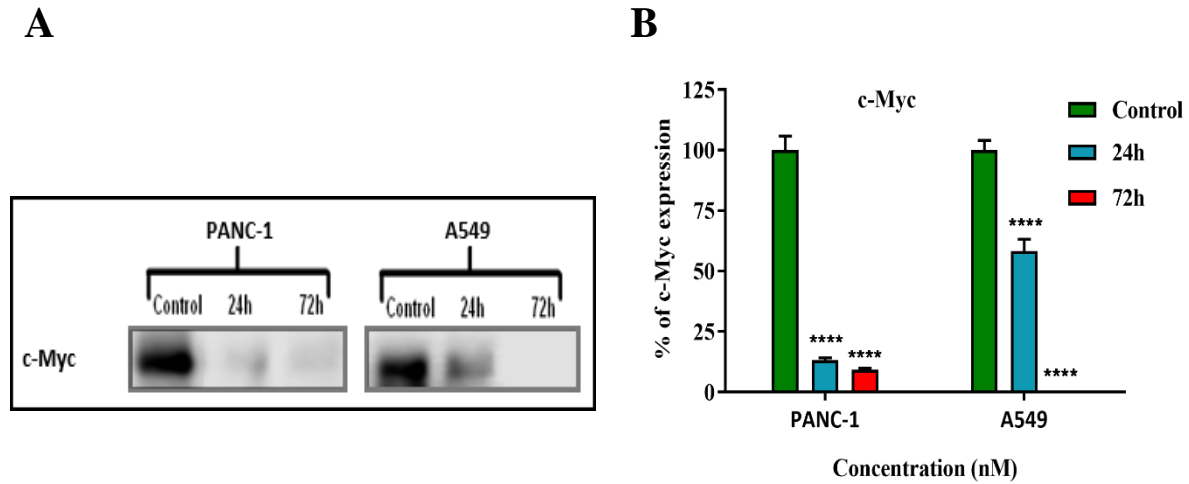


Figure S5. Western blot analysis of c-Myc in PANC-1 and A549 cells (A).

Cells were treated with 2x GI₅₀ CR for 24 h and 72 h. GAPDH was used as an internal control (Fig. 10). (B) Collated densitometric measurement of protein expression levels; time-dependent downregulation of c-Myc was observed at 2 x GI₅₀ after 24 and 72 h treatment (****P < 0.0001 compared to controls, experiment repeated ≥ 3 times).

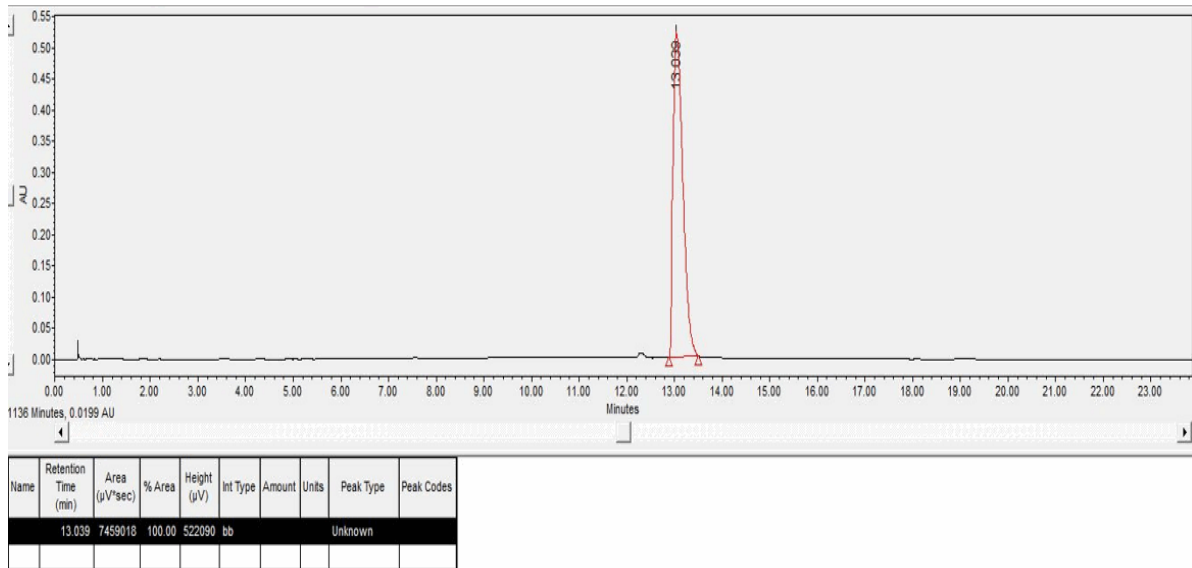


Figure S6. Chromatogram for CR sample, PDA 254 nm.

Total injection volume was 5 μ L (5 mg/mL CR stock solution in ACN). Chromatogram with PDA detection at 254 nm was obtained, which showed a single well resolved peak at Rt 13.04 min. No other significant impurity peaks were detected.